Green reduction of graphene oxide using Rumex vesicarius extracts and study of antibacterial activity

Conference Paper · June 2024

DOI: 10.57647/j.jtap.2024.si-AICIS23.22

2 authors, including:

Ghassan Naeem
University of Anbar
19 PUBLICATIONS **182** CITATIONS

SEE PROFILE

Journal of Theoretical and Applied Physics (JTAP), Special Issue: AICIS'23-Article 22

Proceeding of the 3rd Annual International Conference on Information and Sciences 2023, University of Fallujah, Iraq

https://dx.doi.org/10.57647/j.jtap.2024.si-AICIS23.22

Green reduction of graphene oxide using Rumex vesicarius extracts and study of antibacterial activity

Abdullah Kassar Raja[1,*], Ghassan Adnan Naeem[2]

[1]*Department of Physics, College of Education for Pure Science, University of Anbar, Anbar, Iraq.*
[2]*Department of Medical Physics, College of Applied Science-Hit University of Anbar Hit, Anbar, Iraq.*

[*]**Corresponding author:** abdullah94alobaidi@gmail.com

Original Research

Published online:
15 June 2024

Abstract:

The study examines the in vitro biological responses to reduced graphene oxide (rGO), and looks at how rGO can be synthesized from Rumex vesicarius leaf extract, a more environmentally friendly approach. A range of spectroscopic and microscopic techniques thoroughly describe the environmentally produced rGO. From the XRD spectral data, a clear 2θ increase to 24.25° can be seen, confirming the reduction of graphene oxide (GO) into rGO. Furthermore, FTIR spectra indicate that deoxygenation of GO is indeed successful. Using FESEM, it can be explained how rGO is created through a morphological change in GO, and EDX analysis reveals that there has been an initial decrease from 38% to only 18%. Allowing the biotinylated rGO nanosheets to successfully synthesize Rumex vesicarius, a green reducing agent (i.e., one that acts as an antioxidant), takes advantage of all bioactive compounds in its leaf extract, exerting their individual effects upon it. This bio-reduced rGO also has remarkable antibacterial properties. In particular, it is effective against *Staphylococcus aureus* and *Pseudomonas aeruginosa*. This research is directed to the dire urgency for novel, efficient biomaterials in light of highly infectious pathogenic bacterial strains resistant to traditional antibiotics. They note that cells of bio-reduced rGO have the potential as a medical agent to combat antibiotic resistance, stressing the importance of bio-reduction in current time when there is mounting concern about antimicrobial resistance.

Keywords: Nanobiotechnology; Nanosheets; Rumex vesicarius; EDX analysis; Biological method

1. Introduction

There has been remarkable progress recently in nanobiotechnology, merging nanoscience and biotech. Using phytochemicals to synthesize new types of nanomaterial is an excellent example. The complementary effect of these two branches has enabled the creation of various nanomaterial designs, especially biologically compatible nanometrically with possible medical and pharmaceutical applications [1, 2].

Interestingly, since its discovery in 2004, graphene has become a point of focus for researchers due to the material's characteristics. A single-layer sp^2 hybrid carbon atom arrayed in a hexagonal structure provides high electrical and thermal conductivity together with ample surface area. These exceptional properties make graphene applicable for many other uses as well, such as supercapacitors [3], biosensors, solar cells, catalysts, drug delivery, and water purification systems of various kinds [4].

Many processes have been used to produce graphene, of which the reduction with chemicals (chemical exfoliation) of bleached graphene oxide is recognizable as being simple and scalable. The chemical reducers are key to converting graphene oxide (GO) into just plain old graphene. Prominent chemical-reducing agents are dimethylhydrazine, hydroquinone, sodium borohydride, and hydrazine hydrate [5]. On the other hand, chemical-reducing agents are of course not environmentally friendly products. Consequently, there has been a trend toward finding sustainable and environmental reduction methods that do less harm to the planet (such as those based on plants) [6].

Eco-friendly reductants Reducing agents can be split into organic acids, microorganisms, sugars, proteins, and amino acid-reducing agents. To overcome the environmental threat of chemical-reducing agents, industries have turned their

attention to finding sustainable alternatives. Reduction solutions using plant extracts are now being explored all over industry and academia alike [7, 8]. Research in biomedical nanotechnology has taken off over the past decade, setting new milestones for the production of green nanoparticles. Synthesized nanoparticles of phytochemicals are garnering growing attention for their anti-inflammatory, antibacterial, and anticancer properties. A clean, cheap, and sustainable technique, biosynthesis of nanoparticles offers several advantages over other biological techniques.

Whereas plant extracts have indeed proved effective at reducing graphene oxide, no one has tried using Rumex vesicarius as a green reducer for synthesizing reduced graphene oxide (rGO). The goal of this study is to explore the phytochemical properties of R. vesicarius leaf extract for graphene oxide reduction, as well as a complete analysis and description of rGO produced by such methods, along with an assessment of its antibacterial activity. This study also adds to the developing understanding of sustainable and green ways of synthesizing nanomaterials that have applications in biomedicine.

2. Experimental

2.1 Materials and chemicals

The following materials were procured and utilized without additional purification: graphite powder (99 percent pure, mesh size 325), potassium permanganate ($KMnO_4$), sodium nitrate ($NaNO_3$), sulfuric acid H_2SO_4), and hydrochloride acid. The use of deionized water (DI) to make the graphene oxide (GO). Hummer's technique was used to achieve success in the production of GO nanosheets.

2.2 Synthesis of GO nanosheets

Graphite powder was the starting material for the production of GO nanosheets, using a modified Hummer method [9, 10]. By employing this method, graphite, H_2SO_4, after which the temperature must be kept below 20 °C, and by adding oxidizing $KMnO_3$ and $NaNO_3$ agents have been where oxidized graphite to a compound of graphitic carbon. This mixture was then stirred for 18 hours at a temperature of 35 °C. Afterward, 3 milliliters of 30% H_2O_2 were added in drops, and the resultant suspension turned a bright yellow. This was then centrifuged at 5000 rpm for 15 minutes, after which HCl (3 mL) and distilled water were used to wash until the (pH = 7). Next, the product was dried in a 40 °C oven for 24 hours. The dried GO was re-thawed in detergent water (1 mg/mL) to ensure that it was homogeneously distributed.

2.3 Plant material preparation

The producers thoroughly washed mature leaves of R. vesicarius with distilled water and dried them at 50 °C. They then took the dried leaves and passed them through a home blender before storing the resulting powder in an air-tight box.

2.3.1 Preparation of R. vesicarius leaf extract

Preparation of the R. vesicarius leaf extract included mixing 15 gm of finely ground leaves with 150 mL distilled water and boiling for half an hour at a temperature of 100 °C. The mixture was filtered after one hour through a 0.45 μm filter to extract the desired materials, which were then kept at 4 °C.

2.3.2 Reduced synthesis of graphene oxide using leaf extracts

rGO was synthesized from GO precursors with R. vesicarius leaf extracts acting as catalysts. At first, 50 mL of solution containing 1 mg/ mL of GO was raised in pH = 10 by using NaOH (0.1N), and then the leaf extracts were added. After 15 minutes of constant stirring at 90 °C, it was centrifuged for 15 minutes. The resulting black precipitate, or rGO was dried for 24 hours at 60 °C. The reduction of oxygen in GO is evident from the change in color from yellow-brown to black, is shown in Fig. 1.

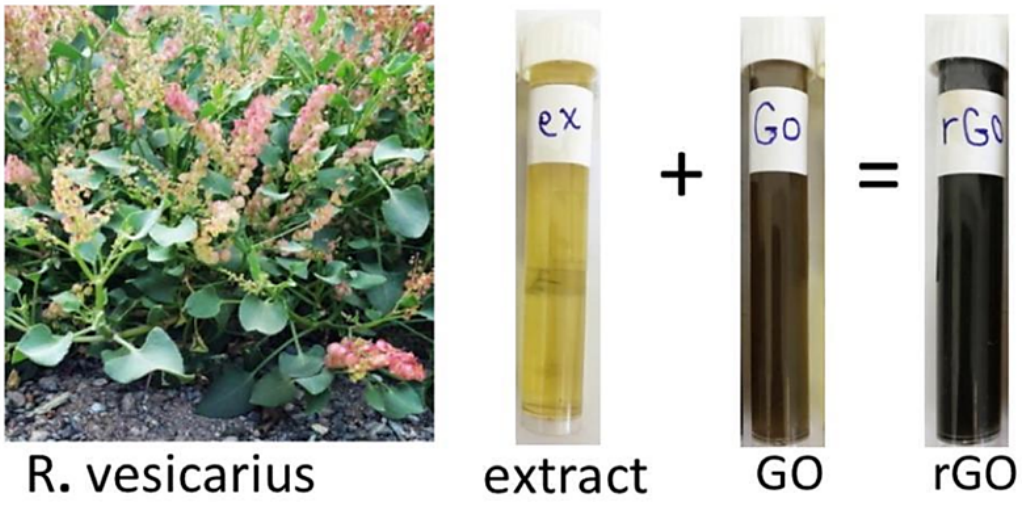

Figure 1. Visualizing the reduction: from yellow brown to black this is the sequence of transition colors that appear when graphene oxide (GO) loses oxygen.

3. Characterization of synthesized GO nanosheets

To gain an understanding of the synthesized graphene oxide (GO) nanosheets, numerous analytical methods were employed in a comprehensive analysis of structural and crystalline characteristics as well as morphology.

3.1 Fourier transform infrared spectroscopy (FTIR)

A Shimadzu FTIR 8400s instrument from Japan was used to do the analysis. Using wavelengths from 500 to 4000 cm^{-1}, the functional groups in both types of compound were studied. From this analysis, the chemical composition and bonding arrangements of a newly synthesized nanomaterial could be determined.

3.2 X-ray Diffraction (XRD)

Crystalline properties of GO and rGO were analyzed by XRD with Rigaku-Ultima IV made in Japan. The diffraction patterns and crystallographic structure of the nanosheets were studied using nickel-filtered Cu-Kα (λ = 0.154 nm). Further study of structural transformations through the reduction process was possible using XRD analysis.

3.3 Field emission scanning electron microscope (FE-SEM)

The morphologies of the GO and rGO were confirmed by an FESEM test using a German-made Carl Zeiss SUPRA55 instrument. By using this high-resolution imaging technique, scientists were able to observe the topography of the nanosheets 'surface, their size, and shape. The structural transformation that takes place after the reduction of the nanomaterial was a topic inherently suited for study by FESEM.

3.4 Energy dispersive X-ray diffraction (EDX)

Synthesized nanosheets were analyzed through Energy Dispersive X-ray diffraction (EDX) and scanning electron microscopy to determine their elemental composition. This analysis made use of a MIRA3 TESCAN instrument from the Czech Republic. EDX analysis also gave quantitative data on the relative proportions and spatial distribution of elements in the nanomaterial, as well.

Such multi-technique characterization gives a clear picture of the structure and attributes (crystalline, morphological) of synthesized nanomaterials. Such observations not only help to understand the reduction process but also explain many of the properties of reduced graphene oxide.

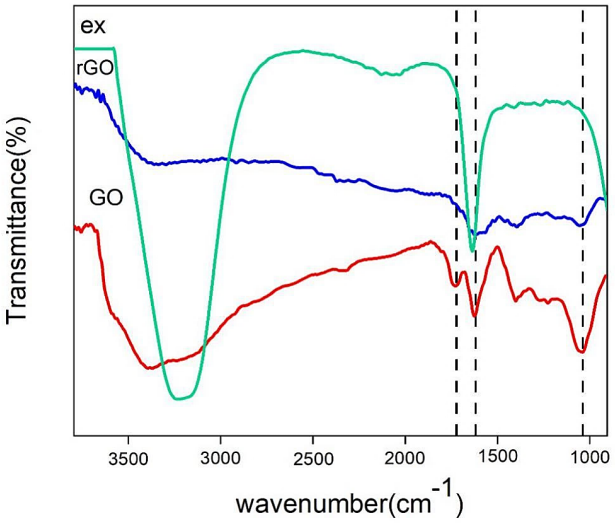

Figure 2. FTIR spectra of the GO ,ex and rGO.

4. Results and discussion

4.1 FTIR analysis

The plant extract of Rumex vesicarius (ex), graphene oxide (GO), and reduced graphene oxide (rGO) were sent for analysis using Fourier transform infrared spectroscopy, which was used to identify their functional groups. The FTIR spectra of these samples are shown in Fig. 2.

Plant extract (ex) noteworthy peaks found in the spectrum of plant extracts include 3392 cm^{-1} (alcohols and phenols) and 1652 cm^{-1} (aromatic, C=C). Also, the presence of carboxylic acid-related alcohols or ethers (C-O stretch at 1268 cm^{-1}) is supported by a smaller peak, which appears when this frequency is probed.

For the GO spectrum, peaks at 1044 cm^{-1} (C-O), 1366 cm^{-1} (O-H), 1642 cm^{-1} (C=C), and 1723 cm^{-1} (C=O) are typical of spectra obtained for bonds within that molecule's polymer; its characteristic four main peak wavelengths were reported in reference articles. The broad peak at 3432 cm^{-1} is due to water adsorbed on the surface and (O-H) stretch vibrations of the (–COOH) functional groups. That suggests the extensive production of oxygen-containing functional groups during the oxidation process [11, 12].

From a comparison of the rGO spectrum to the spectrum for pure GO, it can be seen that peaks designated (OH), (C=O), and (C-O) are somewhat less intense than in unreduced samples. This reduction will result in rGO that has lost the oxygen-containing functional groups from its structure. The fact that these peaks have lessened intensity in the spectrum of reduced rGO suggests a successful reduction, which supports the idea that oxygen functionalities can be removed during green reduction using Rumex vesicarius leaf extract. This reduction improves the properties of rGO, including its conductivity and other physical characteristics. It also makes it suitable for many applications [13–15]. The changes in the FTIR spectra are consistent with expected variations in the chemical composition of nanomaterials after reduction.

4.2 X-ray diffraction

We used X-ray diffraction (XRD) to study the crystallinity, phase composition, and lattice parameters of graphene oxide (GO) and reduced graphene oxides. XRD spectra for both the GO and rGO are revealed in Fig. 3.

The XRD spectrum of the GO has a clear single peak at 10.72°, with d-spacing (082 nm), corresponding to its (00l) plane. The d-spacing increase is related to the intercalation of water molecules between graphite layers and oxygen functional groups initiated by the reaction. After Rumex vesicarius extract is sprayed on the water of a GO solution, there appears another broad peak centered 2θ = 24.25° and

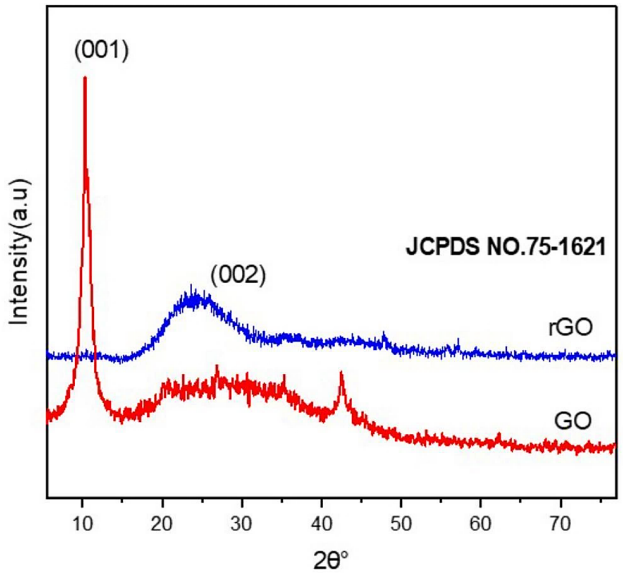

Figure 3. Diffraction patterns of GO and rGO.

d-spacing (0.487 nm), which is attributed to the (002) plane and JCPDS Card No. is matched with 75-1621 [16]. A peak shift and the broader peak are attributable to restacking of graphene sheets by reduction, with incorporation into an amorphous structure. The lower d-spacing (0.487 nm) in rGO is indicative of the removal of oxygen functional groups, according to studies by other authors that argue for a foil-like structure at this point [14, 15].

The crystal size (D) of GO and rGO was calculated using the Scherer-Debye equation [17]:

$$D = \frac{K\lambda}{\beta \cos\theta} \tag{1}$$

where λ: is the X-ray wavelength of (0.15406 nm), K: is a constant equal to (0.89) approximately, β: is the radial value resulting from multiplying of full width at half maximum (FWHM) by (π/180) and θ: is the Bragg angle. The microstrain (ε) of the lattice was calculated by the equation [18]:

$$\varepsilon = \frac{\beta_{0.5}}{4\tan\theta} \tag{2}$$

The dislocation intensity (δ) was determined using the formula [2]:

$$\delta = \frac{1}{D^2} \tag{3}$$

The surface area ($S.A.$) of GO and rGO was computed using the equation [19]:

$$S.A. = \frac{6}{D_{av}\rho} \tag{4}$$

The density of Go and rGo are ~ 1.8 g/cm^3 & $1.50 - 1.70$ g/cm^3.

Error! Reference source not found. gives the predicted crystal size, estimated with the use of the Scherer-Debye equation, as well as the values for the dislocation density and the micro-compliance of the produced nanocrystals.

The results of the reduction process on the important structural parameters for both graphene oxide (GO) and reduced graphene oxide (rGO) nanosheets are presented in **Error! Reference source not found**. There is a clear decrease in crystalline size, D nm, with an accompanying increase in dislocation density (δ), surface area ($S.A.$), and microstress values (ε). This indicated that this modulation of the structural material properties was due to reduction. The reduction also reduces the rate of crystallization, leading to a corresponding decrease in the size of crystal molecules. This reduction affects the rhythms of crystal growth, which causes crystallization to be smaller in rGO than in GO. In addition, the surface area of each crystal is increased by this reduction. With a decrease in functional oxygen groups, the surface becomes more porous-which increases rGO's surface area. This increase in surface area is closely connected with a greater micro-ductility the crystal will have acquired as a result of exposure to stress during reduction. At the same time, it gives us an idea of how micro stresses have increased. This could be traced back to changes in crystals as a result of being subjected to stress by reduction processes. With this increased micro-ductility, stress is more absorbed by the crystal, and dislocation density falls.

4.3 FE-SEM analysis

The morphology of our composite graphene oxide (GO) and reduced graphene oxide (rGO), as analyzed by field emission scanning electron microscopy, is shown in Fig. 4. The wrinkled and wavy shape of the sheets was confirmed by FE-SEM analysis, which also revealed their exfoliation. You can readily see the sheets, with their surface roughness, perhaps due to interactions between these GO layers, carboxyl groups, and H_2O molecules. These surface features align with what should be observed from exfoliated GO samples.

The results of FE-SEM analysis, in comparison, show that the rGO retains a significant portion of folded and coiled sheets with fewer stacked individual sheets. The reduction

Table 1. Microstructral parameters of Go and rGo.

Sample	2θ	(hkl)	β	d_{hkl}	D (nm)	$(S.A.)$ $\times 10^3$ cm^2/g	(δ) $\times 10^{11}$/cm^2	(ε) $\times 10^{-3}$
Go	10.72	(001)	0.022	0.82	6.26	0.532	0.0255	0.0586
rGo	24.25	(002)	0.0725	0.487	1.935	1.823	0.267	0.0843

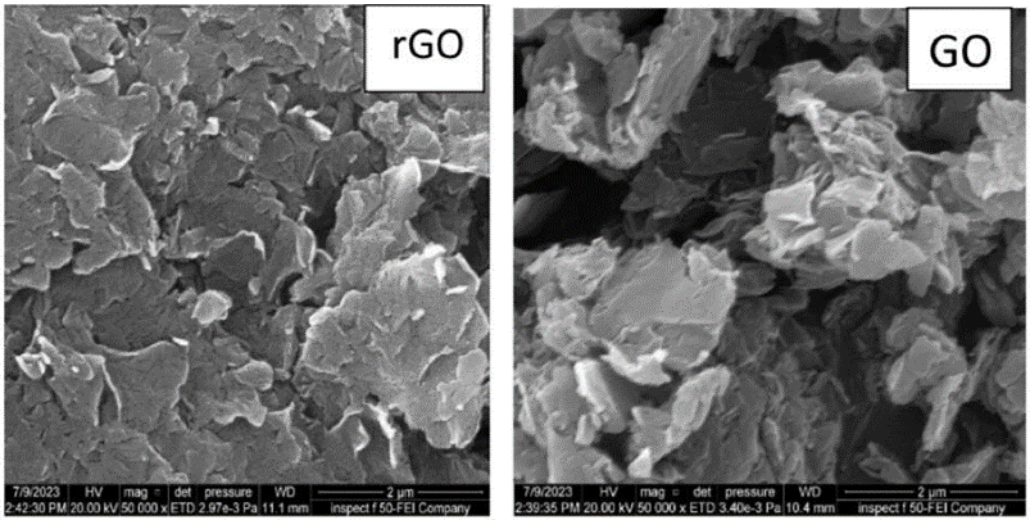

Figure 4. FE-SEM images of GO and rGO.

process removes oxygen-containing functional groups and lets interlayer Van der Waals forces join the rGO sheets together to stack. This structural change is perfectly cocksound with the XRD results, which demonstrate that rGO has a smaller interlayer distance than pure GO. The role of induced transformation sheets piled up by the coiling process points to an increase within rGO in intermolecular forces between sheets, one possible factor responsible for its apparent change in morphology.

The structural changes that accompany the reduction process yielded through an FE-SEM analysis offer important insights into the transformation of functional groups in GO. The partially unfolded and coiled sheet-like structure of the rGO, combined with the narrower interlayer spacing, confirms that they have successfully stripped off oxygen functional groups to restore some normal bonds in reduced graphene oxide [16].

4.4 EDX analysis

Energy dispersive X-ray spectroscopy (EDX) was used to examine the chemical makeup of graphene oxide and reduced graphene oxide. Fig. 5 shows the EDX spectra of GO and rGO.

The EDX spectrum of the base GO shows a high concentration of oxygen (O), which is evidence that oxidation has been successful. A high level of oxygen is, as expected from an oxidized graphite species (graphite plus O functional groups), the case.

By contrast, the EDX spectrum of rGO reveals a corresponding large decrease in oxygen content, which indicates that reduction has been effective. The higher carbon-to-oxygen (C:O) ratios in rGO compared to GO support the reduction effectiveness, as the C/O atomic ratio increased from 1.55 to 4.04. This reduction is due to the use of Rumex extract as a green reducing agent. In c. R vesicarius also contains an environmentally friendly reducing agent that can facilitate the removal of oxygen-containing functional groups, leading to reduced carbon content in rGO [19].

A decrease in oxygen content based on EDX data values, the O concentration fell from 38.3% (GO) to only 19.2% after r GO preparation (rGO). The marked decrease in oxygen level and increase in the carbon-to-oxygen ratio shows that R. vesicarius is an efficient, environmentally friendly reduction agent for the synthesis of reduced graphene oxide. The quantified results from EDX analysis focus on the elemental composition of GO and rGO, highlighting that Rumex vesicarius extract can effectively reduce graphite oxide. Such a reduction in the oxygen content of EDX would

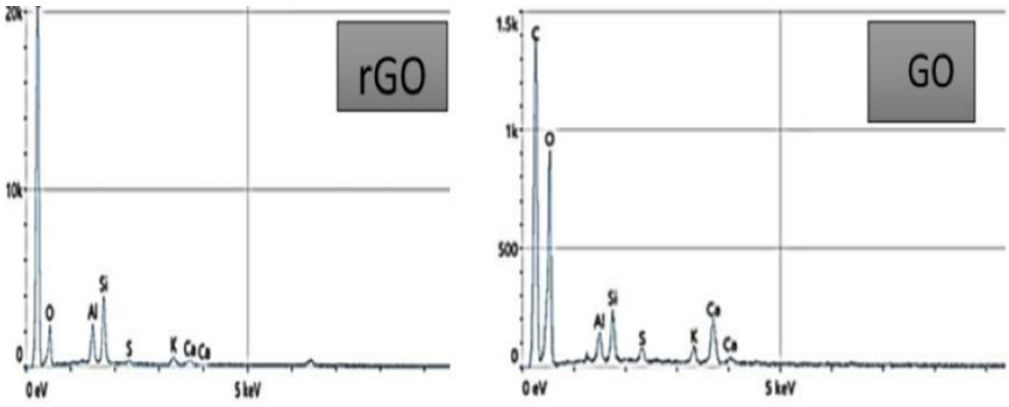

Figure 5. EDX spectrum of GO and rGO.

be evidence that R. vesicarius, which had been used as a reducing agent, was indeed environmentally benign.

4.5 Antibacterial activity of rGO nanosheets

Because they are antibacterial, graphene materials show broad-spectrum viability against gram-positive and gram-negative bacteria [20], a very special feature that increases their applicative potential. This study aimed to test the antibacterial effectiveness of rGO nanosheets prepared using Rumex vesicarius. Different concentrations (0.25, 0.5, 1, and 2 mg/mL) were tested for inhibition zones against gram-positive bacteria *Staphylococcus aureus* (*S.aureus*) and gram-negative bacteria *Pseudomonas aeruginosa* (*P.aeruginosa*). The use of the Mueller-Hinton agar diffusion method involved dropping 40 μL solution containing rGO into each well and incubation for 24 hours at a temperature of 37 °C. Measurement results indicate that the higher its concentration, the more effective rGO nanosheets are at inhibiting bacteria in a given area, as shown in Error! Reference source not found. (*S. aureus*) and (*P. aeruginosa*) bacteria can be observed in Fig. 6.
Several theories have been put forward to explain how graphene nanosheets achieve their antibacterial properties. Their exact mechanisms involve physical disruption or structural damage to bacterial cell walls and membranes, as well as the detaching of bacteria from their environments; these events trigger the production of reactive oxygen species (ROS) [21, 22].
These zones of growth inhibition clearly show that the Rumex vesicarius-derived rGO nanosheets are a powerful antimicrobial for both gram-positive and gram-negative bacteria. Furthermore, its increased antibacterial effect at higher doses indicates that the rGO produced by this environmentally friendly bioelectric method causes destabilization of cell membranes and, subsequently, death to bacteria. The results indicate the antibacterial activity of biosynthesized rGO at varying concentrations, suggesting that it could be an effective antimicrobial agent. Its concentration-dependent growth inhibition zone indicates that it increases the effectiveness of rGO in disrupting bacterial cell membranes.

5. Conclusion

Graphene oxide (GO) was successfully prepared using the Hummer method based on a chemical route. A green reduction method using Rumex vesicarius leaf extract was then used to reduce graphene back into rGO effectively. This is the first method of using Rumex vesicarius leaf extract for direct reduction to a tar-like GO. The GO was synthesized from graphene oxide, and the reduction process and comprehensive chemistry characterization (FTIR, XRD, FE-SEM & EDX) confirmed its successful availability. These analytical results collectively show that rGO's oxygen functional groups were greatly decreased

Figure 6. Zone of inhibition image of (*S. aureus* and *P. aeruginosa*) bacteria.

Table 2. Inhibition zone for (*S.aureus*) and (*P.aeruginosa*).

Concentration	Mean zone of inhibition (mm)	Mean zone of inhibition (mm)
Antibacterial agent	*S.aureus* gram-positive	*P.aeruginosa* gram-negative
0.25 mg/ml	15	9
0.5 mg/mL	20	10
1 mg/mL	21	12
2 mg/mL	24	16

by the process of green reduction, which proves Rumex vesicarius leaf extract served as a successful reducing agent. Especially noteworthy is that the study shows R. vesicarius leaf extract to be a surprisingly sustainable and environmentally friendly alternative means of reducing cholesterol, eliminating dependence on harsh chemical reagents in developed countries-which are hard-pressed for eco-friendly alternatives. Add to this that the tests for antibacterial activity showed rGO produced with Rumex vesicarius leaf extract has strong inhibitory action against both gram-positive and gram-negative bacteria. This result leads me to believe that biosynthesized rGO is an effective antibacterial agent. Finally, this work points out that the industrial manufacture of rGO using Rumex vesicarius leaf extract is both effective and environmentally friendly. The above characteristics of rGO (with lowered oxygen functional groups and heightened antibacterial effects) have promoted it as an important new material in green nanotech. The use of plant extracts for the green synthesis of graphene materials not only opens up novel directions in nanotech but also comports with sustainable and environmentally friendly practices to bring about new possibilities for functional biomaterials.

Authors Contributions
Authors have contributed equally in preparing and writing the manuscript.

Availability of data and materials
Data presented in the manuscript are available via request.

Conflict of Interests
The author declare that they have no known competing financial interests or personal relationships that could have appeared to influence the work reported in this paper.

References

[1] W. Chen, L. Huang, and B. Zhou. "Green supported silver nanoparticles over modified reduced graphene oxide: Investigation of its antioxidant and anti-ovarian cancer effects.". *Open Chem*, , 2023. DOI: https://doi.org/10.1515/chem-2022-0348.

[2] M. N. Owaid, G. A. Naeem, R. F. Muslim, and R. S. Oleiwi. "Synthesis, characterization and antitumor efficacy of silver nanoparticle from Agaricus bisporus pileus, Basidiomycota.". *Walailak J. Sci. Technol*, , 2020. DOI: https://doi.org/10.48048/wjst.

[3] A. K. Geim and K. S. Novoselov. "The rise of graphene.". *Nat. Mater*, , 2007. DOI: https://doi.org/10.1038/nmat1849.

[4] V. B. Mbayachi, E. Ndayiragije, T. Sammani, S. Taj, and E. R. Mbuta. "Graphene synthesis, characterization and its applications: A review.". *Results Chem*, , 2021. DOI: https://doi.org/10.1016/j.rechem.

[5] D. Behar, T. Rajh, Y. Liu, J. Connell, V. Stamenkovic, and J. Rabani. "Unusual reduction of graphene oxide by titanium dioxide electrons produced by ionizing radiation: reaction products and mechanism.". *J. Phys. Chem*, , 2020. DOI: https://doi.org/10.1021/acs.jpcc.9b11042.

[6] N. Thiyagarajulu, S. Arumugam, A. L. Narayanan, T. Mathivanan, and R. R. Renuka. "Green synthesis of reduced graphene nanosheets using leaf extract of tridax procumbens and its potential in vitro biological activities.". *Biointerface Res. Appl. Chem*, , 2020. DOI: https://doi.org/10.33263/BRIAC113.99759984.

[7] K. K. H. De Silva, H.-H. Huang, R. K. Joshi, and M. Yoshimura. "Chemical reduction of graphene oxide using green reductants.". *Carbon N. Y*, , 2017. DOI: https://doi.org/10.1016/j.carbon.

[8] Y. Wang, P. Zhang, C. F. Liu, L. Zhan, Y. F. Li, and C. Z. Huang. "Green and easy synthesis of biocompatible graphene for use as an anticoagulant. ". *RSC Adv*, , 2012. DOI: https://doi.org/10.1039/C2RA00841F.

[9] H. Altaee, H. A. H. Alshamsi, and B. A. Joda. "Reduced graphene oxide supported palladium nanoparticles as an efficient catalyst for aerobic oxidation of benzyl alcohol. ". *AIP Conference Proceedings*, , 2020. DOI: https://doi.org/10.1063/5.0027427.

[10] H. A. Alshamsi, N. A. A.-B. Jaber, and S. H. A. Altaa. "Facile green synthesis of reduced graphene oxide in L-cysteine solution and its structural, morphological, optical and thermal characteristics.". *Journal of Physics: Conference Series*, , 2021. DOI: https://doi.org/10.1088/1742-6596/1999/1/012016.

[11] M. Ebrahimi Naghani, M. Neghabi, M. Zadsar, and H. Abbastabar Ahangar. "Synthesis and characterization of linear/nonlinear optical properties of graphene oxide and reduced graphene oxide-based

zinc oxide nanocomposite.". *Sci. Rep*, , 2023. DOI: https://doi.org/10.1038/s41598-023-28307-7.

[12] N. Thiyagarajulu and S. Arumugam. " Green synthesis of reduced graphene oxide nanosheets using leaf extract of lantana camara and its in-vitro biological activities. ". *J. Clust. Sci*, , 2021. DOI: https://doi.org/10.1007/s10876-020-01814-7.

[13] M. N. Rani, M. Murthy, N. S. Shree, S. Ananda, S. Yogesh, and R. Dinesh. "Cuprous oxide anchored reduced graphene oxide ceramic nanocomposite using Tagetes erecta flower extract and evaluation of its antibacterial activity and cytotoxicity. ". *Ceram. Int*, **1003**, 2019. DOI: https://doi.org/10.1016/j.ceramint.2019.04.195.

[14] M. T. H. Aunkor, I. M. Mahbubul, R. Saidur, and H. S. C. Metselaar. "The green reduction of graphene oxide.". *Rsc. Adv.*, **1029**:363–372, 2016. DOI: https://doi.org/10.1039/C6RA03189G.

[15] M. J.-Y. Tai et al. "Green synthesis of reduced graphene oxide using green tea extract. ". *AIP Conference Proceedings*, , 2018. DOI: https://doi.org/10.1063/1.5080845.

[16] P. Punniyakotti, R. Aruliah, and S. Angaiah. "Facile synthesis of reduced graphene oxide using Acalypha indica and Raphanus sativus extracts and their in vitro cytotoxicity activity against human breast (MCF-7) and lung (A549) cancer cell lines.". *3 Biotech*, , 2021. DOI: https://doi.org/10.1007/s13205-021-02689-9.

[17] M. A. Rabeea et al. "Phytosynthesis of Prosopis farcta fruit-gold nanoparticles using infrared and thermal devices and their catalytic efficacy.". *Inorg. Chem. Commun.*, , 2021. DOI: https://doi.org/10.1016/j.inoche.2021.108931.

[18] G. A. Naeem, R. F. Muslim, M. A. Rabeea, M. N. Owaid, and N. M. Abd-Alghafour. "Punica granatum L. mesocarp-assisted rapid fabrication of gold nanoparticles and characterization of nano-crystals. ". *Environ. Nanotechnology, Monit. Manag*, , 2020. DOI: https://doi.org/10.1016/j.enmm.2020.100390.

[19] G. A. Naeem, M. A. Majeed, and S. G. Khalil. "Improvement of silver nanoparticles biosynthesized using various quantity of Ruta leaf extract. ". *Int. J. Nanosci*, , 2023. DOI: https://doi.org/10.1142/S0219581X23500606.

[20] B. Meka Chufa, B. Abdisa Gonfa, T. Yohannes Anshebo, and G. Adam Workneh. "A novel and simplest green synthesis method of reduced graphene oxide using methanol extracted Vernonia Amygdalina: large-scale production. ". *Adv. Condens. Matter Phys*, , 2021. DOI: https://doi.org/10.1155/2021/6681710.

[21] M. F. Almamad and N. H. Aldujaili. "Characterization of graphene oxide reduced by Bacillus clausii and its activity against MDR uropathogenic isolates.". *IOP Conference Series: Earth and Environmental Science*, , 2021. DOI: https://doi.org/10.1088/1755-1315/790/1/012044.

[22] A. Al-Jumaili, S. Alancherry, K. Bazaka, and M. V Jacob. "Review on the antimicrobial properties of carbon nanostructures.". *Materials (Basel)*, , 2017. DOI: https://doi.org/10.3390/ma10091066.